nature nanotechnology

ARTICLES

PUBLISHED ONLINE: 18 JANUARY 2016 | DOI: 10.1038/NNANO.2015.313

Additive interfacial chiral interaction in multilayers for stabilization of small individual skyrmions at room temperature

C. Moreau-Luchaire[1], C. Moutafis[2,3]*, N. Reyren[1]*, J. Sampaio[1†], C. A. F. Vaz[2], N. Van Horne[1], K. Bouzehouane[1], K. Garcia[1], C. Deranlot[1], P. Warnicke[2], P. Wohlhüter[2,4], J.-M. George[1], M. Weigand[5], J. Raabe[2], V. Cros[1]* and A. Fert[1]

Facing the ever-growing demand for data storage will most probably require a new paradigm. Nanoscale magnetic skyrmions are anticipated to solve this issue as they are arguably the smallest spin textures in magnetic thin films in nature. We designed cobalt-based multilayered thin films in which the cobalt layer is sandwiched between two heavy metals and so provides additive interfacial Dzyaloshinskii–Moriya interactions (DMIs), which reach a value close to 2 mJ m^{-2} in the case of the Ir|Co|Pt asymmetric multilayers. Using a magnetization-sensitive scanning X-ray transmission microscopy technique, we imaged small magnetic domains at very low fields in these multilayers. The study of their behaviour in a perpendicular magnetic field allows us to conclude that they are actually magnetic skyrmions stabilized by the large DMI. This discovery of stable sub-100 nm individual skyrmions at room temperature in a technologically relevant material opens the way for device applications in the near future.

To process and store the continually increasing quantity of information constitutes a major challenge that is the target of many research programmes. The hard-disk drives, in which information is encoded magnetically, allow the storage of zettabytes (10^{21}) of information, but this technology will soon reach its limits. An up-and-coming avenue appeared with the discovery of magnetic skyrmions[1,2], that is, spin windings that can be localized within a diameter of a few nanometres and can move like particles[3]. These magnetic solitons, remarkably robust against defects because of their topology[4], are promising as being the ultimate magnetic bits to carry and store information in magnetic media. Furthermore, the topology of the skyrmions[5] appears to underline other important features, such as their current-induced motion (caused by a small direct current (d.c.)), which is crucial for applications, and also the existence of a specific component in the Hall effect[6–8] that can be used for an electrical readout of the information carried by nanoscale skyrmions[9]. We proposed recently that these skyrmions could be used in future information-storage and processing devices[3].

The existence of the skyrmion spin configuration was predicted theoretically about 30 years ago[1], but it was only recently that skyrmion lattices were observed in crystals with non-centrosymmetric lattices, in particular in B20 structures such as MnSi[8,10–12], FeCoSi[13] or FeGe[7] crystals. Although skyrmions have only been observed below room temperature (r.t.) in such compounds, a very recent publication by Tokunaga *et al.*[14] reported the observation of skyrmion lattices above r.t. in β-type CuZnMn alloys. In 2011, skyrmions were also identified in monolayers (Fe) or bilayers (Fe|Pd) of ferromagnetic metals with out-of-plane magnetization deposited on heavy-metal substrates, Ir(111)[15,16]. Thin magnetic films appear to be more compatible with technological developments, although the observation of nanoscale skyrmions in thin films has been limited, until recently, to low temperatures[16]. The study of these new magnetic phases associated with chiral interactions generated a very strong interest in the community of solid-state physics.

The magnetic skyrmions are, in most cases, induced by chiral interactions of the Dzyaloshinskii–Moriya (DM) type, which result from spin–orbit effects in the absence of inversion symmetry. The Hamiltonian of the DM interaction (DMI) between two neighbouring atomic spins S_1 and S_2 can be expressed as $H_{DMI} = \mathbf{D}_{12}(\mathbf{S}_1 \times \mathbf{S}_2)$ where $\mathbf{D}_{12}$ is the DM vector (top of Fig. 1a)[17]. In this work, we focus on ultrathin magnetic systems in which the DMI results from the breaking of the inversion symmetry at the interface of the magnetic layers and heavy metals that provide a strong spin–orbit coupling and lead to DMI magnitudes nearly as large as the Heisenberg exchange[16]. In such a case, the DM vector $\mathbf{D}_{12}$ is perpendicular to the $\mathbf{r}(S_1) - \mathbf{r}(S_2)$ vector ($\mathbf{r}(\cdot)$ being the position vector) and gives rise to cycloidal skyrmionic configurations called Néel skyrmions. During the submission of our article, Chen *et al.*[18] reported a r.t. skyrmion in a Fe|Ni system with a magnetic exchange layer that provides an effective magnetic field to stabilize the skyrmion phase, and Jiang *et al.*[19] observed micron-sized skyrmions at r.t. in a system composed of a single-nanometre-thick CoFeB film in contact with Ta film, which presumably resulted from a small DMI. Our main goal in the work reported here is to extend the generation of interface-induced skyrmions from monolayer-thick magnetic films[15,16] to multilayers by stacking layers of magnetic metals and non-magnetic heavy metals (for example, Pt and Ir) so as to induce a much larger DMI at all the magnetic interfaces (Fig. 1a) and allow the observation of small skyrmions at r.t. The advantages of such innovative multilayered systems are twofold. First, we anticipate that the thermal

[1]Unité Mixte de Physique, CNRS, Thales, Univ. Paris-Sud, Université Paris-Saclay, Palaiseau 91767, France. [2]Swiss Light Source, Paul Scherrer Institute, 5232 Villigen, Switzerland. [3]School of Computer Science, University of Manchester, Manchester M13 9PL, UK. [4]Laboratory for Mesoscopic Systems, Department of Materials, ETH Zurich, 8093 Zurich, Switzerland. [5]Max Planck Institute for Intelligent Systems, 70569 Stuttgart, Germany. †Present addresses: Laboratoire de Physique des Solides, CNRS, Univ. Paris-Sud, Université Paris-Saclay, Orsay 91405, France. *e-mail: christoforos.moutafis@manchester.ac.uk; nicolas.reyren@thalesgroup.com; vincent.cros@thalesgroup.com

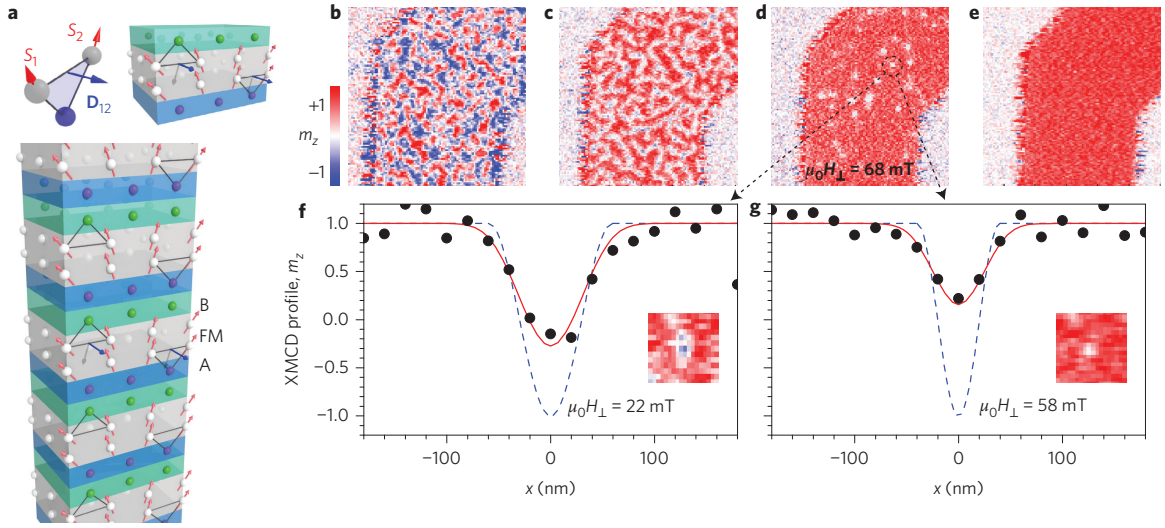

Figure 1 | Interfacial DMI in asymmetric magnetic multilayers. a, Top left: the DMI for two magnetic atoms (grey spheres) close to an atom with a large spin–orbit coupling (blue sphere) in the Fert–Levy picture[14]. Top right: zoom-in on a single trilayer composed of a magnetic layer (FM, grey) sandwiched between two different heavy metals A (blue) and B (green) that induce the same chirality (same orientation of **D**) when A is below and B above the magnetic layer. Bottom: a zoom-in on an asymmetric multilayer made of several repetitions of the trilayer. **b**–**e**, A 1.5 × 1.5 μm^2 out-of-plane magnetization (m_z) map obtained by STXM on a (Ir|Co|Pt)$_{10}$ multilayer at r.t. for applied out-of-plane magnetic fields of 8 (**b**), 38 (**c**), 68 (**d**) and 83 (**e**) mT. **f**, Experimental X-ray magnetic circular dicroism (XMCD) signal through a magnetic circular domain (skyrmion) as observed at 22 mT (black dots). The blue dashed curve is the magnetization profile of an ideal 60-nm-diameter skyrmion and the red curve derives from the model described in the text. **g**, Same type of data at 58 mT and the corresponding simulation of a 40-nm-diameter skyrmion. The images and data of **f** and **g** result from the same skyrmion evolution in the field. The actual image size of the insets is 360 nm.

stability of skyrmions can be greatly improved simply because of the increase of their magnetic volume, as it turns out that for our samples the same magnetic texture extends vertically throughout the multilayer (exactly as for coupled domain walls in similar types of multilayers[20]). Second, the choice of two different heavy metals A and B sandwiching each magnetic layer (ferromagnetic layer (FM), Fig. 1a) can lead to additive interfacial chiral interactions that increase the effective DMI of the magnetic layer if the two heavy materials induce interfacial chiral interactions of opposite symmetries and parallel **D** (see Fig. 1a).

The first important conclusion drawn from the analysis of our observations is that the presence of circular-shaped domains in the 30–90 nm size range cannot be accounted for by dipolar interaction[21–24]. As our micromagnetic simulations also show that these small circular-shaped domains can only be explained by the presence of a large DMI that imposes a winding number equal to one, we identify them as skyrmions. We also show that both the size of the circular-shaped domains and their field dependence are consistent with simulations of skyrmions. The size of the skyrmions in this article, between 30 and 90 nm depending on the field, corresponds to the size that can be imaged with our experimental technique, but we predicted[25] recently that, with the same DMI, even smaller sizes can be obtained by tuning the other parameters, such as perpendicular magnetic anisotropy or the thickness of the ferromagnetic layers. The stabilization in multilayers and at r.t. of individual nanoscale magnetic skyrmions induced by large chiral interactions represents the most significant result of this work. Given the important features of magnetic skyrmions associated with their topological character (small size, easier current-induced propagation, smaller sensitivity to defects and so on), this advance represents a definite breakthrough in the route to highly integrated skyrmion-based memory devices[3].

Multilayers with additive chiral interaction at interfaces

The prototype of the multilayered systems that we studied is presented in Fig. 1a. The samples grown by sputtering are stacks of ten repetitions of an Ir|Co|Pt trilayer, each trilayer being composed of a 0.6-nm-thick Co layer sandwiched between 1 nm of Ir and 1 nm of Pt: Pt10|Co0.6|Pt1|(Ir1|Co0.6|Pt1)$_{10}$|Pt3 (numbers are thickness in nm). The choice of the two heavy materials, that is, Pt and Ir, was guided by recent experiments on asymmetric domain-wall propagation[26,27] as well as by recent *ab initio* predictions of opposite DMIs for Co on Ir and Co on Pt[28], which correspond to additive DMI at the two interfaces of the Co layers sandwiched between Ir and Pt. In addition to these Ir|Co|Pt asymmetric multilayers, we prepared reference samples of Pt|Co|Pt with symmetric interfaces, a type of structure investigated in previous studies that showed a non-complete cancellation of the DMI at the Pt/Co and Co/Pt may lead to a small, but non-negligible, global DMI[27,28]. Details about the growth conditions and the characterization of their magnetic properties are presented in Methods.

We present next the micromagnetic simulations[30,31] for the simplest assumption in which the experimental magnetization M and magnetic anisotropy K are distributed uniformly in the ten 0.6-nm-thick Co layers and equal to zero elsewhere. The simulations were performed for one of these Co layers with the experimental values of M and K. Moreover, the potential impact of the exchange stiffness A of the magnetic Co layer was investigated by performing a series of micromagnetic simulations with different amplitudes of A. Dipolar interactions are always included. In a second series of simulations (see the Supplementary Information), to take into account that part of the experimental values of M and K comes from the proximity-induced magnetism in Pt or Ir, we evaluated the maximum possible changes of our results induced by such spreading of the magnetization by assuming a dilution of M, K and A inside the multilayer. This leads to a slightly different estimate of the interfacial DMI magnitude without affecting our main conclusion.

Magnetization mapping in asymmetric multilayers

The mapping of the out-of-plane component of the magnetization in our Ir|Co|Pt multilayers and its evolution as a function of

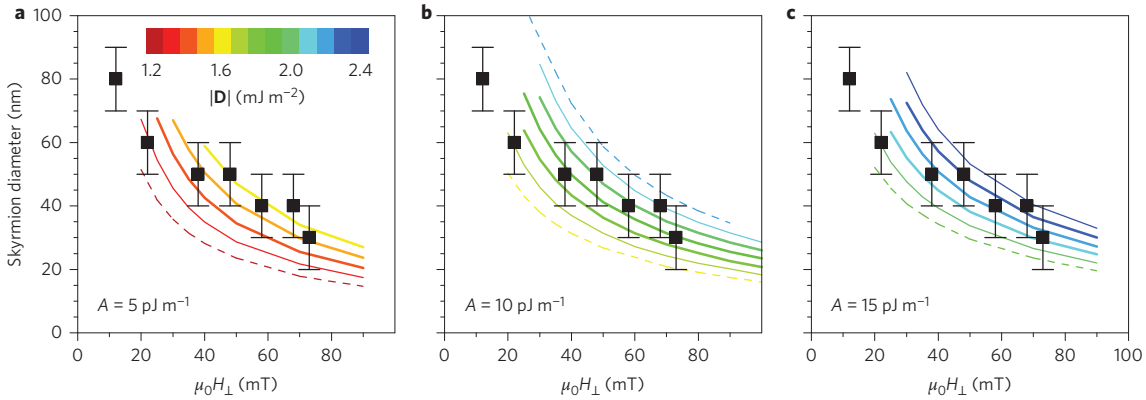

Figure 2 | Skyrmion diameter as a function of the external out-of-plane magnetic field $H_\perp$. Experimental diameters (squares) can be compared with micromagnetic simulations for different values of $|\mathbf{D}|$ (lines) and different values of the exchange interaction A (panels). Simulations were obtained in the case that gives a lower bound to the experimental $|\mathbf{D}|$ value (no exchange coupling between magnetic layers). For $A = 5$ pJ m^{-1}, circular skyrmions are not stable for $|\mathbf{D}| \geq 1.7$ mJ m^{-2} and deform into labyrinthic worm-like structures. The deviation of the data compared with the simulations at a low field can be explained by the interaction with the other domains.

the external perpendicular field was performed by scanning transmission X-ray microscopy (STXM) on samples grown on Si_3N_4 membranes and measuring the dichroic signal at the Co L_3 edge. In Fig. 1b–e, we display experimental images obtained at different external out-of-plane magnetic field ($H_\perp$) values. After saturation at a large negative field and inversion of the field, we first observed a domain configuration (Fig. 1b at 8 mT) that combines some labyrinth-shaped domains with other domains having almost a circular shape. When the field was increased to $\mu_0 H_\perp = 38$ mT, the magnetic domains favoured by the field extend (red domains in Fig. 1c). Before complete saturation of the magnetization is reached (see Fig. 1e at $\mu_0 H_\perp = 83$ mT), Fig. 1d (at 68 mT) shows a typical field range up to about 80 mT in which isolated magnetic domains of an approximately circular shape persist in an almost totally perpendicularly polarized sample. As the STXM probes the total thickness, these images correspond to an average of the magnetic configuration throughout the ten magnetic layers. As we mainly observed two opposite contrast amplitudes (corresponding to $m_z = \pm 1$), we conclude that these magnetic configurations, worms or circular-shaped domains from Fig. 1b–d, run throughout the magnetic thickness of the multilayer[20].

We now focus on the dimension of these circular-shaped domains as well as on their increase when $H_\perp$ is decreased. We show that both are consistent with a large DMI value and the corresponding skyrmion modelling. As shown in Fig. 1f,g, we can determine precisely the size evolution of selected isolated nanoscale domains at decreasing fields from the analysis of the STXM images (see the Supplementary Information). Results for the Ir|Co|Pt multilayers are presented as squares in Fig. 2. We find that the diameter of the circular-shaped domains goes from about 30 nm at $\mu_0 H_\perp = 73$ mT to 80 nm at $\mu_0 H_\perp = 12$ mT. At a lower field (closer to zero), the magnetic contrast evolves towards worm-like domains from which a proper diameter can no longer be defined. We emphasize that the diameter of the circular-shaped domains (around 80 nm) that we observe at very low field values remains extremely small compared with the usual values (at the least, larger than 800 nm with the parameters of our films) observed in classic bubble systems[21–23] in which the driving mechanism for bubble stabilization is the dipolar interaction.

To obtain more insights into the actual interaction at play in our multilayered Ir|Co|Pt systems, we compare in Fig. 2 the experimental data for the field dependence of the size of the circular-shaped domains with micromagnetic simulations of DMI-induced skyrmions. First, in these simulations using as inputs the experimental magnetization and anisotropy constant, dipolar interactions can typically never stabilize a classic bubble below the micrometre range. A second important issue for the determination of the DMI magnitude is to evaluate the impact of the value of the exchange constant A in Co. A is, indeed, particularly difficult to estimate for ultrathin magnetic layers and has not been obtained experimentally here. However, it was observed recently in a similar stacking of Co thin films with heavy metals[32] that A is markedly influenced by the surface/volume ratio and evolves from 15 pJ m^{-1} for multilayers with 7-nm-thick Co layers (a typical value for bulk Co) down to about 7 pJ m^{-1} for 2-nm-thick Co layers. Consequently, we decided to compare the experimental results with three series of simulations obtained with different exchange constants that ranged from 5 to 15 pJ m^{-1}. The simulated diameters versus $H_\perp$ curves that correspond to different values of the DMI are compiled in Fig. 2. It is important that, with the DMI taken into account and whatever the value of A, bubble-like configurations relax for $|\mathbf{D}| \geq 1$ mJ m^{-2} in a stable configuration of an isolated skyrmion having a winding number $|W|$ equal to 1, where $W = (1/4\pi) \int \mathbf{s}(\partial_x \mathbf{s} \partial_y \mathbf{s})\, dx dy$, $\mathbf{s}$ being the normalized local magnetization (see, for example, Büttner *et al.*[24]). With the smallest exchange constant, $A = 5$ pJ m^{-1}, isolated skyrmions are not stable in our range of magnetic fields for $|\mathbf{D}|$ values larger than 1.6 pJ m^{-1} (see Fig. 2a). Thus, we consider that a reasonable value for the actual exchange constant in our asymmetric multilayers is close to 10 pJ m^{-1}. For this intermediate value (see Fig. 2b), the best agreement with the experimental size and its variation with field is found for $|\mathbf{D}| = 1.9 \pm 0.2$ mJ m^{-2}. This large DMI is comparable, for example, with that derived recently in Pt|Co|AlO_x trilayers from asymmetric domain-nucleation experiments[33], domain-wall annihilation[34], non-reciprocal spin wave propagation[35] and scanning nanomicroscopy[36]. This DMI is in good agreement with recent theoretical predictions that add the DMI magnitudes predicted for Pt|Co (three monolayers) and Ir|Co (three monolayers)[28]. Actually, this range of DMI values is, indeed, close to optimal for the stabilization of isolated skyrmions (and so of isolated magnetic bits) instead of skyrmion lattices[25,37]. Finally, our approach is along the lines of the experimental characterization of skyrmions developed by Romming *et al.*[38], in which the evolution of the size and shape of skyrmions as a function of the magnetic field (using the model developed in Braun[39]) is proposed to compare experimental spin-polarized scanning transmission microscopy images with theory.

In addition to measurements on asymmetric multilayers, we performed a similar analysis with STXM images obtained on symmetric Pt|Co|Pt systems (see the Supplementary Information).

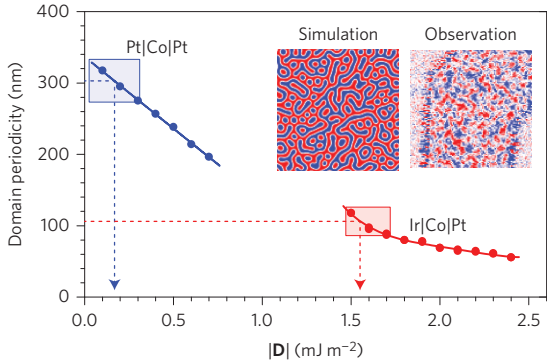

Figure 3 | Micromagnetic simulations and experimental measurements of mean domain-width evolution with DMI after demagnetization. Comparing the simulations with the experimental domain-width value (dotted horizontal line) allows us to estimate $|\mathbf{D}|$(Ir|Co|Pt) = 1.8 ± 0.2 mJ m^{-2} and $|\mathbf{D}|$(Pt|Co|Pt) = 0.2 ± 0.2 mJ m^{-2}. The box height represents the error margins on the experimental domain-size evaluation; its width gives the resulting error on $|\mathbf{D}|$ for the used simulation parameters. The inset shows a simulated worm pattern for $|\mathbf{D}|$ = 1.6 mJ m^{-2} in Ir|Co|Pt (1.5 × 1.5 μm^2) and a corresponding experimental observation at the same scale (using the same colour code as in Fig. 1).

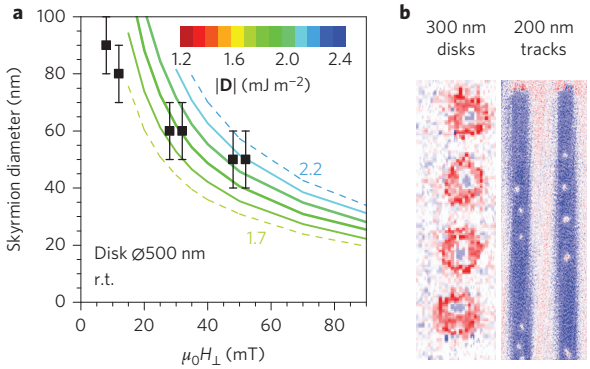

Figure 4 | Evolution of the skyrmion size in patterned nanoscale disks and tracks. a, Magnetic field evolution of the skyrmion size derived from micromagnetic simulations realized for A = 10 pJ m^{-1} (lines for different $|\mathbf{D}|$ values) and sizes of the observed skyrmions (squares) for 500-nm-diameter disks. **b**, R.t. out-of-plane magnetization map of an array of 300-nm-diameter disks with an out-of-plane external field of $\mu_0 H_\perp$ = 8 mT, and two 200-nm-wide tracks at $\mu_0 H_\perp \approx$ 55 mT that display several isolated skyrmions.

The best fit for the size and field dependence of circular-shaped domain configurations is obtained with DMIs that are small but non-negligible. Indeed, it is known that the different structures of the two interfaces in Pt|Co|Pt-like trilayers induce a non-zero DMI[27,29].

To confirm the large DM magnitude in Ir|Co|Pt multilayers, we developed a second approach to estimate it from the analysis of the STXM images at remanence. This method relies on the quantitative analysis of the mean width of the perpendicular magnetic domains. From the images obtained at zero field after demagnetization, shown as an inset in Fig. 3, we measured the average domain width to be 106 ± 20 nm for the Ir|Co|Pt multilayers. The same analysis of similar images for the symmetric Pt|Co|Pt multilayers led to a mean domain width of 303 ± 30 nm. In Fig. 3, these experimental values are compared with those obtained in a series of micromagnetic simulations as a function of the DMI, which allows an estimation of $|\mathbf{D}|$. The material parameters used in these simulations are the same as those that gave Fig. 2b. From this second approach we find that the DMI is about 1.6 ± 0.2 mJ m^{-2} for the asymmetric Ir|Co|Pt multilayers or 0.2 ± 0.2 mJ m^{-2} for the symmetric Pt|Co|Pt sample, and thus close to the values derived from the field dependence of the skyrmion size. Once again, we emphasize that the domain width found in Pt|Co|Ir, in the 100 nm range at zero field, cannot be expected with only dipolar interactions[21].

As mentioned above, we also evaluated how our estimation of the DMI is modified if we take into account the proximity-induced magnetization of Ir and Pt (Supplementary Information). We find that, in this case, the DM magnitude from the asymmetric multilayers is about 1.4 ± 0.3 mJ m^{-2}, the actual value probably being between this latter value and 1.6 ± 0.2 mJ m^{-2} given above. In consequence, all these results converge to a very large interfacial DMI, which enables the observation of skyrmions in technologically relevant systems of magnetic multilayers.

Room temperature isolated skyrmion in disks

As described in the previous section, we found from two independent analyses of the magnetic configurations that very large DMI and skyrmions exist at r.t. in asymmetric (Ir|Co|Pt)$_{10}$ multilayered films. Here we demonstrate that isolated nanoscale skyrmions can be stabilized at r.t. in nanodisks and nanostrips patterned in our multilayers by electron-beam lithography and ion-beam etching. Figure 4a shows the field dependence of the diameter of an approximately circular domain located close to the centre of a 500-nm-diameter disk, and this dependence is compared, as we did in the first section, with that obtained in micromagnetic simulations. Even though the agreement is not as good as that in the extended films shown in Figs 1 and 2, especially in the low-field region, again a major outcome of these simulations is that it is not possible to stabilize any bubble-like domain in submicrometre-sized disks without introducing large DM values of at least 1.5 mJ m^{-2}. As the winding number of the simulated circular domains is, after stabilization, always equal to one, we can conclude that the experimental images correspond to nanoscale skyrmions with a chirality fixed by the sign of D. Figure 4b shows STXM images of 300 nm disks and tracks 200 nm wide with even smaller skyrmions that are stable down to very small fields (~8 mT) of dimensions that range from 90 nm close to a zero field to 50 nm in an applied field. That the observed skyrmion diameter does not depend significantly on the disk diameter was expected from our previous numerical study[25] in which it depends rather on the effective ratio between the DM and exchange interactions, as long as the DM magnitude remains smaller than the threshold value that corresponds to negative domain-wall energy. During the submission of this work, and also in multilayers, Woo *et al.*[40] reported the r.t. observation of multiple skyrmions of relatively large diameter (around 400 nm) in disks of diameter 2 μm patterned in Pt|Co|Ta multilayers.

Conclusion

Our r.t. observation of individual sub-100 nm skyrmions that are produced in magnetic multilayers by a strong and additive interfacial chiral interaction represents the main achievement of this work. Ten repetitions of the Pt|Co|Ir unit are enough to stabilize firmly the skyrmions against thermal fluctuations at r.t. We showed previously[25] that the size of such interface-induced skyrmions (down to 30 nm in the present series) could be reduced even more by tuning the magnetic anisotropy and described how they could be nucleated by spin injection and displaced by the spin Hall effect of the Pt layers. We believe that this experimental breakthrough can be a robust basis for the development of skyrmion-based devices for memory and/or logic applications, as well

as the starting point of further fundamental studies on the very rich physics of skyrmions.

Methods

Methods and any associated references are available in the online version of the paper.

Received 15 July 2015; accepted 30 November 2015; published online 18 January 2016

References

1. Bogdanov, A. & Yablonskii, A. Thermodynamically stable 'vortices' in magnetically ordered crystals. *JETP Lett.* **68,** 101–103 (1989).
2. Bogdanov, A. N. & Rößler, U. K. Chiral symmetry breaking in magnetic thin films and multilayers. *Phys. Rev. Lett.* **87,** 037203 (2001).
3. Fert, A., Cros, V. & Sampaio, J. Skyrmions on the track. *Nature Nanotech.* **8,** 152–156 (2013).
4. Nagaosa, N. & Tokura, Y. Topological properties and dynamics of magnetic skyrmions. *Nature Nanotech.* **8,** 899–911 (2013).
5. Braun, H. J. Topological effects in nanomagnetism: from superparamagnetism to chiral quantum solitons. *Adv. Phys.* **61,** 1–112 (2012).
6. Mühlbauer, S. *et al.* Skyrmion lattice in a chiral magnet. *Science* **323,** 915–919 (2009).
7. Huang, S. X. & Chien, C. L. Extended skyrmion phase in epitaxial FeGe(111) thin films. *Phys. Rev. Lett.* **108,** 267201 (2012).
8. Ritz, R. *et al.* Formation of a topological non-Fermi liquid in MnSi. *Nature* **497,** 231–234 (2013).
9. Kiselev, N. S., Bogdanov, A. N., Schäfer, R. & Rößler, U. K. Chiral skyrmions in thin magnetic films: new objects for magnetic storage technologies? *J. Phys. D* **44,** 392001 (2011).
10. Neubauer, A. *et al.* Topological Hall effect in the α phase of MnSi. *Phys. Rev. Lett.* **102,** 186602 (2009).
11. Pappas, C. *et al.* Chiral paramagnetic skyrmion-like phase in MnSi. *Phys. Rev. Lett.* **102,** 197202 (2009).
12. Tonomura, A. *et al.* Real-space observation of skyrmion lattice in helimagnet MnSi thin samples. *Nano Lett.* **12,** 1673–1677 (2012).
13. Yu, X. Z. *et al.* Real-space observation of a two-dimensional skyrmion crystal. *Nature* **465,** 901–904 (2010).
14. Tokunaga, Y. *et al.* A new class of chiral materials hosting magnetic skyrmions beyond room temperature. *Nature Commun.* **6,** 7238 (2015).
15. Heinze, S. *et al.* Spontaneous atomic-scale magnetic skyrmion lattice in two dimensions. *Nature Phys.* **7,** 713–718 (2011).
16. Romming, N. *et al.* Writing and deleting single magnetic skyrmions. *Science* **341,** 636–639 (2013).
17. Fert, A. & Levy, P. M. Role of anisotropic exchange interactions in determining the properties of spin-glasses. *Phys. Rev. Lett.* **44,** 1538–1541 (1980).
18. Chen, G., Mascaraque, A., N'Diaye, A. T. & Schmid, A. K. Room temperature skyrmion ground state stabilized through interlayer exchange coupling. *Appl. Phys. Lett.* **106,** 242404 (2015).
19. Jiang, W. *et al.* Blowing magnetic skyrmion bubbles. *Science* **349,** 283–286 (2015).
20. Baltz, V., Marty, A., Rodmacq, B. & Dieny, B. Magnetic domain replication in interacting bilayers with out-of-plane anisotropy: application to Co/Pt multilayers. *Phys. Rev. B* **75,** 014406 (2007).
21. Malozemoff, A. P. & Slonczewski, J. C. in *Magnetic Domain Walls in Bubble Materials* (ed. Wolfe, R.) Ch. II, III (Academic Press, 1979).
22. Moutafis, C., Komineas, S. & Bland, J. A. C. Dynamics and switching processes for magnetic bubbles in nanoelements. *Phys. Rev. B* **79,** 224429 (2009).
23. Moutafis, C. *et al.* Magnetic bubbles in FePt nanodots with perpendicular anisotropy. *Phys. Rev. B* **76,** 104426 (2007).
24. Büttner, F. *et al.* Dynamics and inertia of skyrmionic spin structures. *Nature Phys.* **11,** 225–228 (2015).
25. Sampaio, J., Cros, V., Rohart, S., Thiaville, A. & Fert, A. Nucleation, stability and current-induced motion of isolated magnetic skyrmions in nanostructures. *Nature Nanotech.* **8,** 839–844 (2013).
26. Kabanov, Y. P. *et al.* In-plane field effects on the dynamics of domain walls in ultrathin Co films with perpendicular anisotropy. *IEEE Trans. Magn.* **46,** 2220–2223 (2010).
27. Hrabec, A. *et al.* Measuring and tailoring the Dzyaloshinskii–Moriya interaction in perpendicularly magnetized thin films. *Phys. Rev. B* **90,** 020402 (2014).
28. Yang, H., Thiaville, A., Rohart, S., Fert, A. & Chshiev, M. Anatomy of Dzyaloshinskii–Moriya interaction at Co/Pt interfaces. Preprint at http://arxiv.org/abs/1501.05511 (2015).
29. Franken, J. H., Herps, M., Swagten, H. J. M. & Koopmans, B. Tunable chiral spin texture in magnetic domain walls. *Sci. Rep.* **4,** 5248 (2014).
30. Donahue, M. J. & Porter, D. G. *OOMMF User's Guide Version 1.0*. Interagency Report NISTIR 6376 (National Institute of Standards and Technology, 1999).
31. Vansteenkiste, A. *et al.* The design and verification of MuMax3. *AIP Adv.* **4,** 107133 (2014).
32. Eyrich, C. *et al.* Effect of substitution on the exchange stiffness and magnetization of Co films. *Phys. Rev. B* **90,** 235408-235419 (2015).
33. Pizzini, S. *et al.* Chirality-induced asymmetric magnetic nucleation in Pt/Co/AlO_x ultra-thin microstructures. *Phys. Rev. Lett.* **113,** 047203 (2014).
34. Hiramatsu, R., Kim, K.-J., Nakatani, Y., Moriyama, T. & Ono, T. Proposal for quantifying the Dzyaloshinskii–Moriya interaction by domain walls annihilation measurement. *Jpn. J. Appl. Phys.* **53,** 108001 (2014).
35. Belmeguenai, M. *et al.* Interfacial Dzyaloshinskii–Moriya interaction in perpendicularly magnetized Pt/Co/AlO_x ultrathin films measured by Brillouin light spectroscopy. *Phys. Rev. B* **91,** 180405(R) (2015).
36. Tetienne, J.-P. *et al.* The nature of domain walls in ultrathin ferromagnets revealed by scanning nanomagnetometry. *Nature Commun.* **6,** 6733 (2015).
37. Rohart, S. & Thiaville, A. Skyrmion confinement in ultrathin film nanostructures in the presence of Dzyaloshinskii–Moriya interaction. *Phys. Rev. B* **88,** 184422 (2013).
38. Romming, N., Kubetzka, A., Hanneken, C., von Bergmann, K. & Wiesendanger, R. Field-dependent size and shape of single magnetic skyrmions. *Phys. Rev. Lett.* **114,** 177203 (2015).
39. Braun, H. J. Fluctuations and instabilities of ferromagnetic domain–wall pairs in an external magnetic field. *Phys. Rev. B* **50,** 16485 (1995).
40. Woo, S. *et al.* Observation of room temperature magnetic skyrmions and their current-driven dynamics in ultrathin Co films. Preprint at http://arxiv.org/abs/1502.07376 (2015).

Acknowledgements

The authors acknowledge B. Sarafimov and M. Bechtel for their technical support at the SLS and Bessy II beamlines. The STXM experiments were performed using the X07DA (PolLux) beamline at the SLS, Paul Scherrer Institüt, Villigen, Switzerland and the Maxymus beamline BESSY II, Adlershof, Germany. The authors acknowledge financial support from the Agence Nationale de la Recherche project ANR-14-CE26-0012 ULTRASKY and from European Union grant MAGicSky No. FET-Open-665095.

Author contributions

N.R., C.M., V.C. and A.F. conceived the project. C.D. and C.M.L. grew the films. C.A.F.V., K.G. and N.R. patterned the samples. C.M., C.M.L., N.R., J.S., N.V.H., C.A.F.V., K.B., P.Wa., P.Wo, M.W., J.R. and V.C. acquired the data at the synchrotrons. C.M.L. and N.R. treated and analysed the data with the help of C.M., P. Wa., and V.C. C.M.L., J.S. and N.R. performed the micromagnetic simulations. C.M.L., N.R., V.C. and A.F. prepared the manuscript. All authors discussed and commented the manuscript.

Additional information

Supplementary information is available in the online version of the paper. Reprints and permissions information is available online at www.nature.com/reprints. Correspondence and requests for materials should be addressed to C.M., N.R. and V.C.

Competing financial interests

The authors declare no competing financial interests.

Methods

The studied samples are Co-based multilayers, which were grown by d.c. sputtering at r.t. under an Ar pressure of about 0.25 Pa on two different substrates: thermally oxidized Si wafer or 200-nm-thick Si_3N_4 membranes. The samples grown on SiO_2 were used to determine the macroscopic magnetic properties of the samples, and those on membranes were used for STXM. A 10-nm-thick buffer made of textured Pt ((111)-oriented face-centred cubic) was deposited first, immediately followed by the growth of a Co(0.6 nm)|Pt(1 nm) bilayer. This first bilayer was used to induce a strong-enough perpendicular magnetization anisotropy. We subsequently grew asymmetric structures (Ir(1 nm)|Co(0.6 nm)|$Pt(1\ nm)_{10}$) or symmetric ones ($Co(0.6\ nm)|Pt(1\ nm)_{10}$). Both types of magnetic multilayers were finally capped by an extra 3-nm-thick Pt layer to prevent oxidation. The magnetic properties of the multilayers grown on SiO_2 were measured by a superconducting quantum interference device or alternating gradient field magnetometry. The saturation magnetization and the effective anisotropy were determined from the magnetization loops with out-of-plane and in-plane magnetic fields. From these measurements, we deduced a saturation magnetization of 0.96 ± 0.10 MA m^{-1} (1.6 ± 0.2 MA m^{-1}) and an effective anisotropy of 0.17 ± 0.04 MJ m^{-3} (0.25 ± 0.07 MJ m^{-3}) for the Ir|Co|Pt (Pt|Co|Pt) system. The configuration of their vertical magnetic domains was also investigated by magnetic force microscopy on the very same multilayers grown by sputtering deposition on an SiO_2/Si substrate rather than on Si_3N_4 membranes. Importantly, we found similar values of the mean domain width for images recorded at zero field after a demagnetization process, which means that the estimated DM magnitudes are equal to those determined by STXM.

The magnetic imaging presented here was realized by scanning transmission X-ray experiments that were performed on two different beamlines: the X07DA (PolLux) beamline at the Swiss Light Source (SLS), Paul Scherrer Institute, Villigen, Switzerland, and the Maxymus beamline BESSY II, Adlershof, Germany. The images were recorded by scanning the multilayers grown on Si_3N_4 membranes with an X-ray beam focused by a Fresnel zone plate, which provided a resolution down to 30 nm. Circular polarized light with normal incidence was used to map the out-of-plane magnetization at the nanoscale based on the X-ray magnetic circular dichroism effect (see Supplementary Figs 1–3). For imaging, we scanned the samples at the Co L_3 edge at 779.95 eV. To obtain quantitative information about the DMI, we analysed the evolution of skyrmion dimensions with the out-of-plane field. The actual diameter of the circular-shaped domains was estimated by a fit of the experimental STXM data with the convolution of a modelled magnetization profile with the idealized Gaussian profile of the X-ray beam (as shown in Fig. 1e,f and Supplementary Fig. 2).

The quantitative estimate of the DMI was obtained by comparison of the experimental results with micromagnetic simulations that were performed using two different solvers, either the object-oriented micromagnetic framework[30] or MuMax3[31], both of which take into account the interfacial DM energy. We checked that both solvers led to strictly equivalent results. To perform these simulations, we had to introduce input material parameters: a saturation magnetization of $M_s = 956$ kA m^{-1} and a uniaxial out-of-plane magnetic anisotropy $K = 717$ kJ m^{-3}. The other parameter is the exchange constant A, which we assumed to be $A = 10$ pJ m^{-1} if not stated otherwise. In the micromagnetic simulation of a skyrmion in a perpendicular magnetic field, we relaxed the state at each magnetic field step starting from an initial state that is already a skyrmion. However, we checked that, with our material properties, trivial bubbles (winding number equals zero) turn into skyrmions or vanish under a high magnetic field (~50 mT).